

The Microscopic Origin of Thermal Cracking in Rocks: An Investigation by Simultaneous Time-of-Flight Neutron Diffraction and Acoustic Emission Monitoring

Philip G. Meredith¹, Kevin S. Knight², Stephen A. Boon¹ and Ian G. Wood¹

Abstract. We demonstrate that neutron diffraction measurements make it possible to quantify elastic strains within the interior of solid samples, and thus have great potential for addressing a wide range of problems connected with the characterization of the mechanical properties of geological materials. We use the time-of-flight neutron diffraction technique, in combination with acoustic emission monitoring, to study the evolution of thermal strain within the interior of samples of a pure quartzite during slow heating, and the onset of the associated thermal cracking. Thermal cracking commences around 180°C when the thermal strain deficit along the *a*-axes of quartz grains induces a thermal stress that is close to the bulk tensile strength of the rock.

Introduction

Elevated temperatures can exert a profound influence on cracking in crustal rocks, especially in regions where high geothermal gradients are associated with relatively low lithostatic stresses; such as mid-ocean ridges, volcanic regions and geothermal regions. Crucially, thermally enhanced cracking can also lead to enhanced permeability and fluid flow (Glover et al., 1995; Jones et al., 1997). However, whilst the thermal expansivity of mineral single crystals has been widely tabulated (e.g. Fei, 1995) and theoretical bounds for thermal expansion of polycrystalline rocks have been investigated (e.g. Walsh, 1973), there remain fundamental gaps in our understanding of the micromechanisms that lead to thermal cracking in rocks. One reason for this is the difficulty of directly measuring the thermally-induced internal strains in rock during heating. Traditional strain measurement techniques provide information only at free surfaces, and this may well not be representative of the strain within the interior of the rock. Previously, it has been possible to monitor thermal cracking in rocks *only indirectly* during heating (e.g. by acoustic emission monitoring; Glover et al., 1995; Jones et al., 1997), or directly by microscopy but *only after cooling* to ambient temperature (e.g. Fredrich & Wong, 1986; Glover et al., 1995).

To study the micromechanics of thermal cracking in detail we require ideally a combination of techniques that can both measure the thermal strain build-up within the interior of the sample volume during heating, and also monitor the onset of the associated thermal cracking. Acoustic emission (AE)

monitoring is a well-established technique for studying microcracking in rocks, and it is now possible to use neutron diffraction measurements to quantify elastic strains within the interior of solid materials (Ezeilo & Webster, 1999). Here we report on the integrated use of these two techniques to investigate the evolution of thermal strain and the onset of thermal cracking in rock samples during heating.

The thermal expansion of a mineral grain in a polycrystalline aggregate is constrained by the expansion of its neighbouring grains and so is different from the unconstrained single crystal value. In order to obtain the polycrystal value it is necessary to quantify the constraint. Experimentally, this means that it be possible to determine the thermally-induced elastic strains in the aggregate, so that the stresses can be calculated. This is difficult because the strains are small, and the interior of samples previously inaccessible to experimental measurement. However, the penetrating nature of neutron radiation, which is typically several orders of magnitude greater than for X-rays, allows the lattice parameters of the minerals making up the rock to be determined within the interior of solid samples. By monitoring the change in lattice parameters, the average elastic strain within the volume element sampled by the neutrons may be determined as a function of temperature. By comparing these lattice parameters with those obtained as a function of temperature for unconstrained single crystals, the constraint offered by neighbouring grains in a polycrystalline aggregate may be quantified.

A New Experimental Approach Combining Neutron Diffraction and Acoustic Emissions

The three main causes of thermal stressing in rocks are; (i) thermal gradients, (ii) thermal expansion mismatch between different mineral phases, and (iii) thermal expansion mismatch between differently oriented grains of the same phase, where that phase has anisotropic thermal expansion. To simplify the problem, we have attempted to eliminate causes (i) and (ii) by heating at a low rate that produced a maximum temperature difference across our samples of only about 1°C, and by using a monomineralic rock. The sample material was the Basal Quartzite from the Cambro-Ordovician Eribol Sandstone formation in north-west Scotland. This is a very pure quartzite (>99% quartz) with a relatively uniform grain size in the range 0.4 to 0.5 mm, and a porosity of 1.6%. Samples comprised either cores of quartzite 12 mm in diameter and 40 mm in length, or quartzite powder, from the same rock, held in a neutron-transparent vanadium can of the same size. In order to ensure that the rock was completely broken into its constituent crystallites, whilst introducing the minimum amount of damage, it was crushed and then wet-ground to -20 µm in a McCrone micronising mill.

¹ Department of Geological Sciences, University College London, UK

² ISIS Science Division, Rutherford Appleton Laboratory, UK

For the experiments reported here we used the high-resolution powder diffractometer (HRPD; Ibberson et al., 1992) at the ISIS Spallation Neutron Source (Wilson, 1990), located at the Rutherford Appleton Laboratory (RAL), U.K. ISIS is a pulsed neutron source, in which polychromatic pulses of neutrons are generated by the collision of high-energy protons with a heavy-metal target. The diffraction patterns were collected with the time-of-flight method; in this technique the detectors are at fixed Bragg angles, since Bragg's Law can be satisfied by the polychromatic nature of the incident radiation. In the case of neutrons, the wavelength is inversely proportional to the velocity and thus proportional to the time of arrival at the detector. HRPD is able to provide a uniquely high resolution for time-of-flight neutron diffraction studies because it is located at the end of a 100m neutron guide (other instruments typically have unguided flight paths of 10 to 20m). The detectors were placed in back-scattering geometry, in an arrangement designed to mirror the Debye-Scherrer rings produced by powder diffraction. This arrangement allows a resolution in lattice spacing ($\Delta d/d$) of 5×10^{-4} to be achieved over the range $0.3\text{\AA} < d < 6.0\text{\AA}$, where Δd is the width at half-maximum of the diffraction peak of lattice spacing, d ; it should be noted, however, that the instrument is capable of determining shifts of peak position to two orders of magnitude better than this. The experiments described here are probably only possible using an instrument of this type, in which data across the chosen range of d -spacings are collected simultaneously (allowing rapid recording of the diffraction patterns), and where the essentially constant resolution allows accurate cell parameters to be determined from strongly diffracting, large d -spacing reflections. To obtain equivalent resolution using angle-dispersive diffraction it would be necessary to measure high-angle (i.e. small d -spacing) reflections. These are generally weak and would lead to greatly increased data collection times.

The experiments were conducted using the "Cryofurnace" sample environment of the HRPD instrument that allows samples to be cooled or heated in a 30 mbar He atmosphere from liquid helium temperatures to close to 300°C. Samples were heated at 2°C/min in 10°C steps from 30°C to 270°C. After each 5 minute heating step, samples were allowed to equilibrate thermally for 10 minutes before neutron counting was started. The diffraction patterns were collected from reflections with d -spacings in the range 0.6 to 2.6 Å, with counting times of approximately 18 minutes for the rock core and 35 minutes for the powdered rock. Samples were held in place in the neutron beam by means of a hollow sample holder, modified to accommodate a stainless steel AE waveguide. Although the use of a waveguide attenuates the signal, all amplitudes are attenuated equally, with no distortion of the signal shape (Meredith & Atkinson, 1983). AE output was recorded continuously throughout each heating experiment.

Data Analysis and Results

To measure the thermal strains, we need to determine the unit cell parameters under the conditions of interest. These were extracted from the diffraction patterns by the Pawley method (Pawley, 1981) using the RAL's suite of programs based on the Cambridge Crystallography Subroutine Library (CCSL; Brown & Matthewman, 1993). This method involves no

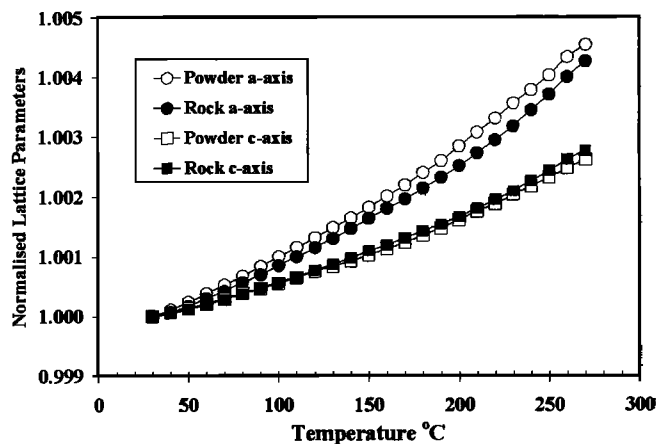


Figure 1: Plot of lattice parameters (normalised to values at 30°C) against temperature for quartzite cores (solid symbols) and quartzite powder (open symbols). The symbol size corresponds to approximately $\pm 10 - 15$ standard deviations and the solid lines are for guidance only.

assumption about the crystal structure, other than that it retains, on average, trigonal symmetry. Strictly, this assumption will not be valid, as each of the crystallites in the rock will be subject to a different set of symmetry-lowering stresses. However, if we assume an average structure of the rock in which each quartz grain exists in a mean field provided by the surrounding quartz grains (a reasonable assumption since the diffraction patterns show no evidence of any preferred orientation), then the average stress on each crystal will have the same symmetry as its thermal expansion. The strain will then also have the same symmetry, which suggests that it is reasonable to process the data assuming trigonal crystals throughout.

Figure 1 shows a plot of the lattice parameters against temperature; normalised to the values at 30°C. Data are plotted for both bulk rock (core) and rock powder, for both the a and c axes of quartz. The estimated standard deviations of the strains, obtained from the results of the Pawley refinements, are similar for both rock and powder and vary little with temperature, having values of 4×10^{-6} for the a -axis and 7×10^{-6} for the c -axis. There are a number of notable features in the data of Figure 1. The bulk rock expands less than the rock powder along the a -axis. This is entirely as expected. Each grain in the unconstrained powder is free to expand fully with increasing temperature, whereas each grain in the bulk rock is partially constrained by the expansion of its neighbouring grains; we term this the internal self-constraint. By contrast, the bulk rock expands more than the rock powder along the c -axis. Again, this is also as expected, and is a consequence of the thermal expansion (α) anisotropy of quartz. The internal self-constraint does not allow the crystals in the bulk rock to expand fully in the high expansion a direction, and the resulting stress produces an additional component of strain in the low expansion c direction. Measurements of the mean thermal expansion coefficients (Bass, 1995) of our quartzite powder (α_1 and α_3) are presented in Table 1, and are consistent with previously reported values.

Figure 2 shows differential thermal strain (powder - rock; data from Figure 1) and cumulative acoustic emission energy plotted against temperature. The differential thermal strain for

Table 1. Experimentally determined mean thermal expansion coefficients for quartz.

α_1 <i>a</i> -axis (10^{-6} K^{-1})	α_3 <i>c</i> -axis (10^{-6} K^{-1})	Temperature ($^{\circ}\text{C}$)	Reference
13	8	Room temp.	Nye (1969)
14.2	8.7	0 - 118	Int'l Tables (1983)
15.0 ± 0.2	8.4 ± 0.1	30 - 130	This study (powder)
18.9 ± 0.4	10.8 ± 0.3	30 - 270	This study (powder)

the *a*-axis is relatively large and positive (compressive), whereas for the *c*-axis it is relatively small and negative (tensile). The cumulative AE energy is seen to increase at an essentially constant rate from ambient temperature to about 180°C. There is then a large burst of activity between 180°C and 200°C, with the peak centered around 190°C. Above this temperature, the AE output decreases again to a steady rate similar to the initial rate. The initial steady rate of activity is considered to be primarily background noise; it is relatively low, essentially constant and there is no mechanical reason for any thermal cracking to occur at these temperatures. Furthermore, similar background rates were measured in the HRPD instrument hall. By contrast, we consider the large burst of activity over the temperature interval 180°C to 200°C to mark the onset of thermally-induced cracking in the quartzite. The steady rate of AE activity observed above 200°C is again interpreted as background activity. This implies that very little, if any, new AE activity is generated in the sample; i.e. this is a period of relative seismic quiescence. A quiescence might be expected if it were associated with a strain relaxation in the sample, such as might occur if the thermal cracking centered around 190°C overcompensated for the thermal strain deficit. The data of Figure 2 does not indicate any strain relaxation following the burst of activity around 190°C; we note, however, that no further thermal cracking (indicated by an increase in the slope of the cumulative AE energy curve) occurs until the temperature reaches 230°C, above which the differential strain on both axes becomes less compressive.

It is illuminating to compare the AE activity in our quartzite with that reported for thermal cracking of a polymineralic rock (La Peyratte granite; Glover et al., 1995). Compared with the quartzite, the AE associated with the onset of thermal cracking in the granite is centered around a lower temperature (100°C as against 190°C), and occurs over a broader temperature interval (50°C as against 20°C). Both of these observations are expected from consideration of the mineralogical composition of the two rocks. Since the granite is polymineralic, thermal expansion mismatches are enhanced relative to the monomineralic quartzite by the different thermal expansion coefficients of the different mineral phases, and the thermal stress required to initiate cracking is generated at a lower temperature. Furthermore, since a range of both mismatch and anisotropy values of thermal expansion coefficients is present in the polymineralic granite, we would also expect the temperature interval over which the initial burst of thermal cracking occurs to be broader.

Discussion

Since our rock comprises >99% quartz, and the diffraction patterns show no evidence of any crystallographically preferred orientation, it is reasonable to assume that the bulk quartzite is essentially isotropic. Hence, neglecting voids, when the whole rock is heated it will expand according to its average thermal expansion coefficient, $\alpha_{av} = (2\alpha_1 + \alpha_3)/3$. Data from Figure 1 show that unconstrained quartz grains heated from 30°C to the temperature corresponding to the onset of thermal cracking (180°C) expand by 2.40×10^{-3} along their *a*-axes and by 1.35×10^{-3} along their *c*-axes. By contrast, grains that are constrained within the quartzite matrix expand on average by 2.14×10^{-3} along their *a*-axes and by 1.42×10^{-3} along their *c*-axes. These differences produce an average strain deficit ($\Delta\epsilon_1$) of 2.6×10^{-4} along *a*-axes and an average strain excess ($\Delta\epsilon_3$) of 0.7×10^{-4} along *c*-axes of the constrained grains at 180°C (Figure 2).

These strain differences are maintained by the rock matrix exerting a stress on individual grains in the quartzite. The candidate mechanisms are either that the matrix exerts a constraining stress (σ_1) along their *a*-axes, that the matrix exerts an extensional stress (σ_3) along their *c*-axes, or both. Our data allow us to determine which is the dominant mechanism by the following analysis. For a grain in the powder, all σ_j 's are equal to zero and the thermal strains are given by: $\epsilon_1^P = \alpha_1 \Delta T$ and $\epsilon_3^P = \alpha_3 \Delta T$, where α_1 and α_3 are the "true" thermal expansion coefficients for quartz (Table 1). By contrast, for a grain in the rock, the stress tensor takes the form: $\sigma_1 = \sigma_2 \neq 0$, $\sigma_3 \neq 0$ and $\sigma_4 = \sigma_5 = \sigma_6 = 0$, assuming, as before, that trigonal symmetry is maintained on average. Hence, $\epsilon_1^R = (s_{11} + s_{12}) \sigma_1 + s_{13} \sigma_3 + \alpha_1 \Delta T$ and $\epsilon_3^R = 2s_{13} \sigma_1 + s_{33} \sigma_3 + \alpha_3 \Delta T$. We now assume (since the material is the same) that α_1 and α_3 are the same for the rock and the powder, i.e. that the difference in apparent thermal expansion coefficients is due to the non-zero σ_j 's. Thus, $\epsilon_1^R = (s_{11} + s_{12}) \sigma_1 + s_{13} \sigma_3 + \epsilon_1^P$ and $\epsilon_3^R = 2s_{13} \sigma_1 + s_{33} \sigma_3 + \epsilon_3^P$. If we now define the differential thermal strain as, $\Delta\epsilon = \epsilon^P - \epsilon^R$, then $(s_{11} + s_{12}) \sigma_1 + s_{13} \sigma_3 + \Delta\epsilon_1 = 0$ and $2s_{13} \sigma_1 + s_{33} \sigma_3 + \Delta\epsilon_3 = 0$. Therefore:

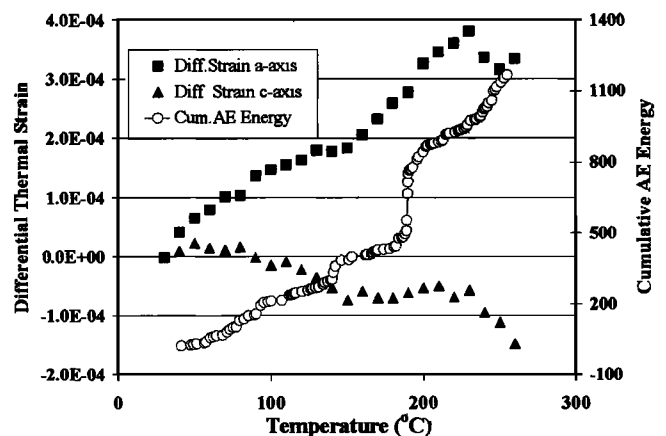


Figure 2: Plot of differential thermal strain (powder - rock) and cumulative acoustic emission energy (arbitrary units) against temperature.

$$\sigma_1 = \frac{s_{33} \Delta \epsilon_1 + s_{13} \Delta \epsilon_3}{2s_{13}^2 - s_{33}(s_{11} + s_{12})} \quad \text{and} \quad \sigma_3 = \frac{(s_{11} + s_{12}) \Delta \epsilon_3 - 2s_{13} \Delta \epsilon_1}{2s_{13}^2 - s_{33}(s_{11} + s_{12})}$$

We can now determine the numerical values of σ_1 and σ_3 at the onset of thermal cracking using the values for $\Delta \epsilon_1$ and $\Delta \epsilon_3$ given above and room-temperature elastic compliances calculated from Bass (1995) ($s_{11} = 1.28 \times 10^{-11} \text{ Pa}^{-1}$, $s_{12} = -0.172 \times 10^{-11} \text{ Pa}^{-1}$, $s_{13} = -0.132 \times 10^{-11} \text{ Pa}^{-1}$ and $s_{33} = 0.974 \times 10^{-11} \text{ Pa}^{-1}$), noting that the temperature dependence of quartz elastic compliances is very small below 300°C (e.g. Carpenter et al., 1998). This gives σ_1 as a compressive stress of 25.1 MPa and σ_3 as a tensile stress of 0.85 MPa. Individual quartz grains will exert an equal and opposite stress on the quartzite matrix. The mechanism responsible for thermal cracking is therefore likely to be splitting of individual quartz grains due to the compressive stress generated along their a -axes, aided by the small tensile stress generated along their c -axes. We have independently measured the tensile strength of our quartzite (using the Brazil disk test) as 22 ± 3 MPa. Thus, the level of thermal stress required to initiate thermal cracking corresponds closely to the bulk tensile strength of the rock.

The lattice parameter measurements reported here enable us to determine the average thermal strain along the a and c axes of all quartz grains in the sample. Similarly, we record the AE energy from all cracking events wherever they occur in the sample. Both techniques therefore monitor average properties of the whole sample and cannot be used to determine either the strain in individual grains or the location of individual cracks. However, the resolution of HRPD is such that it may be possible in future to measure microstrain within the mineral grains from the widths of the diffraction peaks. The program used to analyze the diffraction patterns assumes that the line shape from the sample (i.e. excluding instrumental broadening) is described by a Voigt function. The halfwidths of both the Lorentzian and Gaussian components of the Voigtian include wavelength-dependent terms to simulate the effects of line broadening produced by inhomogeneous strain within the diffracting crystallites. For the powdered rock, neither of these halfwidth components showed any systematic variation with temperature. For the rock core, however, the Gaussian strain-broadening term showed a small but systematic increase as the temperature was raised, as might be expected. Proper quantification of this effect requires analysis of the data using a model allowing anisotropic halfwidths, a facility not yet available within CCSL. We, therefore, consider it beyond the scope of the present work but worthy of future investigation.

Conclusions

This work has demonstrated that a combination of the neutron diffraction and acoustic emission techniques provides a powerful methodology for revealing the microscopic origins of thermal cracking in rocks. On heating, quartz grains constrained within a quartzite aggregate experience a

significantly lower strain along their a -axes than unconstrained single crystals. This thermal strain deficit generates a stress that increases with temperature and leads to the onset of thermal cracking around 180°C when the stress level reaches 25 MPa; a value very close to the tensile strength of the rock.

Acknowledgements

We thank David Dobson for his helpful discussions and Steve Covey-Crump for his thorough and helpful review.

References

- Bass J.D. (1995) Elasticity of minerals, glasses and melts, In: *Mineral Physics and Crystallography: A Handbook of Physical Constants*, ed. T.J. Ahrens, AGU, Washington, 45-63.
- Brown P.J. & Matthewman J.C. (1993) The Cambridge Crystallography Subroutine Lib. - Mark 4 Users' Manual, Report RAL-93-009, Rutherford Appleton Laboratory.
- Carpenter M.A., Salje E.K.H., Graeme-Barber A., Wruck B., Dove M.T. & Knight K.S. (1998) Calibration of excess thermodynamic properties and elastic constant variations associated with the α - β phase transition in quartz, *Am. Mineral.*, **83**, 2-22.
- Ezeilo A.N. & Webster G.A. (1999) Advances in neutron diffraction for engineering residual stress measurements, *Textures and Microstructures*, **33**, 151-171.
- Fei Y. (1995) Thermal expansion, In: *Mineral Physics and Crystallography: A Handbook of Physical Constants*, ed. T.J. Ahrens, AGU, Washington, 29-44.
- Fredrich J.T. & Wong T-f (1986) Micromechanics of thermally induced cracking in three crustal rocks, *J. Geophys. Res.*, **91**, 12,743-12,764.
- Glover P.W.J., Baud P., Darot M., Meredith P.G., Boon S.A., LeRavelec M., Zoussi S. & Reuschlé T. (1995) α/β phase transition in quartz monitored using acoustic emissions, *Geophys. J. Int.*, **120**, 775-782.
- Ibberson R.M., David W.I.F. & Knight K.S. (1992) The high resolution powder diffractometer (HRPD) at ISIS - a user guide, Report RAL-92-031, Rutherford Appleton Laboratory.
- International Tables for X-Ray Crystallography* (1983) Vol. III, Kynoch Press, Birmingham.
- Jones C., Keane G.M.J., Meredith P.G. & Murrell S.A.F. (1997) Fluid permeability measurements of thermally damaged rocks, *Phys. Chem. Earth*, **22**, 13-17.
- Meredith P.G. & Atkinson B.K. (1983) Stress corrosion and acoustic emission during tensile crack propagation in Whin Sill dolerite and other basic rocks, *Geophys. J. R. Astr. Soc.*, **75**, 1-21.
- Nye J.F. (1969) *Physical Properties of Crystals*, Clarendon Press, Oxford.
- Pawley G.S. (1981) Unit-cell refinement from powder diffraction scans, *J. Appl. Crystallogr.*, **14**, 357-361.
- Walsh J.B. (1973) Theoretical bounds for thermal expansion, specific heat, and strain energy due to internal stress, *J. Geophys. Res.*, **78**, 7637-7646.
- Wilson C.C. (1990) ISIS, the UK spallation neutron source - a guided tour, *Neutron News*, **1**, 14-19.

Philip G. Meredith, Stephen A. Boon, and Ian G. Wood, Department of Geological Sciences, University College London, Gower Street, London WC1E 6BT, UK (p.meredith@ucl.ac.uk, s.boon@ucl.ac.uk, ian.wood@ucl.ac.uk)

Kevin S. Knight, ISIS Science Division, Rutherford Appleton Laboratory, Didcot, Oxfordshire OX11 0QX, UK (ksk@isis.rl.ac.uk)

(Received 10 October 2000, revised 21 February 2001, accepted; 27 February 2001)